–

Supporting Information for

Regional Trends and Physical Controls of Streamflow droughts in Tropical Pluvial Flow

Aparna Raut[1], Poulomi Ganguli[1], Rohini Kumar[2], Nagarjuna N. Reddy[1], Bhabani Sankar Das[1] and Thomas Woehling[3]

[1]Indian Institute of Technology Kharagpur, Department of Agricultural and Food Engineering, Kharagpur, India

[2]UFZ-Helmholtz Centre for Environmental Research, Leipzig, Germany

[3]Technische Universität Dresden, Institut für Hydrologie und Meteorologie, Dresden, Germany

Contents of this file

Introduction

In this supporting file, we provide a supplementary text and supplementary figures to support the results presented in the main manuscript.

Text S1

S1.1 Mean Onset and Regularity

For *n* drought events, we determine the mean onset date using the following equations (Burn & Whitfield, 2018; Chen et al., 2012)

$$\bar{X} = \frac{\sum_{i=1}^{n} v_i \cos\theta_i}{\sum_{i=1}^{n} v_i}; \bar{Y} = \frac{\sum_{i=1}^{n} v_i \sin\theta_i}{\sum_{i=1}^{n} v_i} \quad (1)$$

Where, $\overline{X}$ and $\bar{Y}$ are the *x*- and *y*- coordinates of the mean onset date. The equation (1) is derived using the weighted average of drought deficit volume, *v*. Then, we obtain the onset time using mean event angle, $\bar{\phi}$ of individual drought occurrences using the following relationships (2).

$$\bar{\phi} = \begin{cases} tan^{-1}\left(\frac{\bar{Y}}{\bar{X}}\right), if\ \bar{X} > 0 and \bar{Y} > 0 \\ 180 + tan^{-1}\left(\frac{\bar{Y}}{\bar{X}}\right) if\ \bar{X} < 0 and \bar{Y} > 0 \\ 180 + tan^{-1}\left(\frac{\bar{Y}}{\bar{X}}\right), if\ \bar{X} < 0 and \bar{Y} < 0 \\ 360 + tan^{-1}\left(\frac{\bar{Y}}{\bar{X}}\right), if\ \bar{X} > 0 and \bar{Y} < 0 \\ \frac{\pi}{2}, \quad if\ \bar{X} = 0 and \bar{Y} > 0 \\ \frac{3\pi}{2}, if\ \bar{X} = 0 and \bar{Y} < 0 \end{cases} \quad (2)$$

Finally, we obtain the mean onset date as:

$$\omega = tan^{-1}(Mean\ Onset\ Angle)\left(\frac{lenyr}{2\pi}\right) \quad (3)$$

Where, ω is the average date of occurrence of the drought. The regularity ($\overline{r}$) of droughts can be determined from:

$$\bar{r} = \sqrt{\bar{X}^2 + \bar{Y}^2}, \quad 0 \leq \bar{r} \leq 1 \tag{4}$$

Where, r is a dimensionless number. $\bar{r}$ = 0 indicates low regularity, implying droughts are widely spread throughout the year, whereas $\bar{r}$ = 1 denotes high regularity, suggesting droughts at a station occur on the same time of the year. The variability in mean onset timing can be derived using the circular variance (s^2)

$$s^2 = -2ln(\bar{r}) \tag{5}$$

S1.2 Assessment of Inter-regional Differences

We performed the Wilcoxon rank sum test to assess the inter-regional difference between dependence strengths of mean onset time versus deficit volume. For the p-values obtained, we further implemented Bonferroni correction for pairwise comparison and obtained the corrected p-values (Ranstam, 2016) to increase the strengths of the tests. While the Wilcoxon rank-sum test indicates that regions 2 and 3 are geographically distinct at a 5% significance (p-value = 0.04) level, the Bonferroni adjusted p-values for the pairwise comparison demonstrate that inter-regional differences across clusters are statistically indistinguishable (p-value > 0.1) considering the linear-circular dependence between onset time of streamflow droughts and event-specific deficit volume.

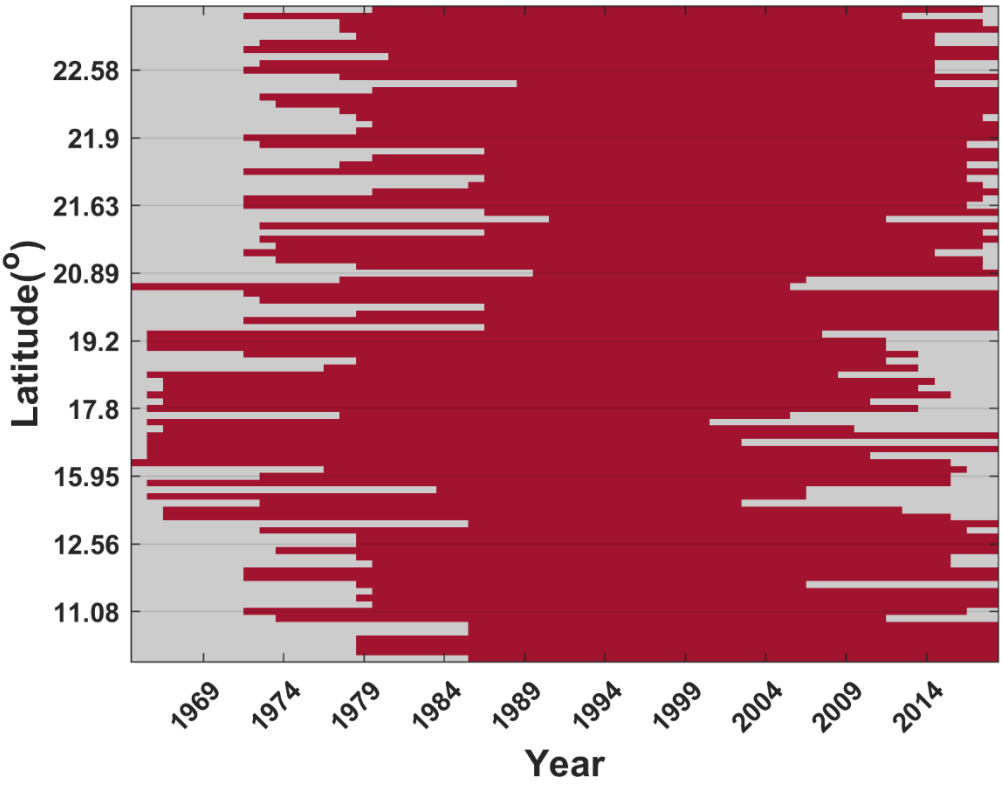

Figure S1. Latitudinal profile of streamflow record availability. The x-axis represents the starting and ending year, whereas the y-axis shows the corresponding latitude of all 97 stream gauges. The red shades indicated the period of records availability.

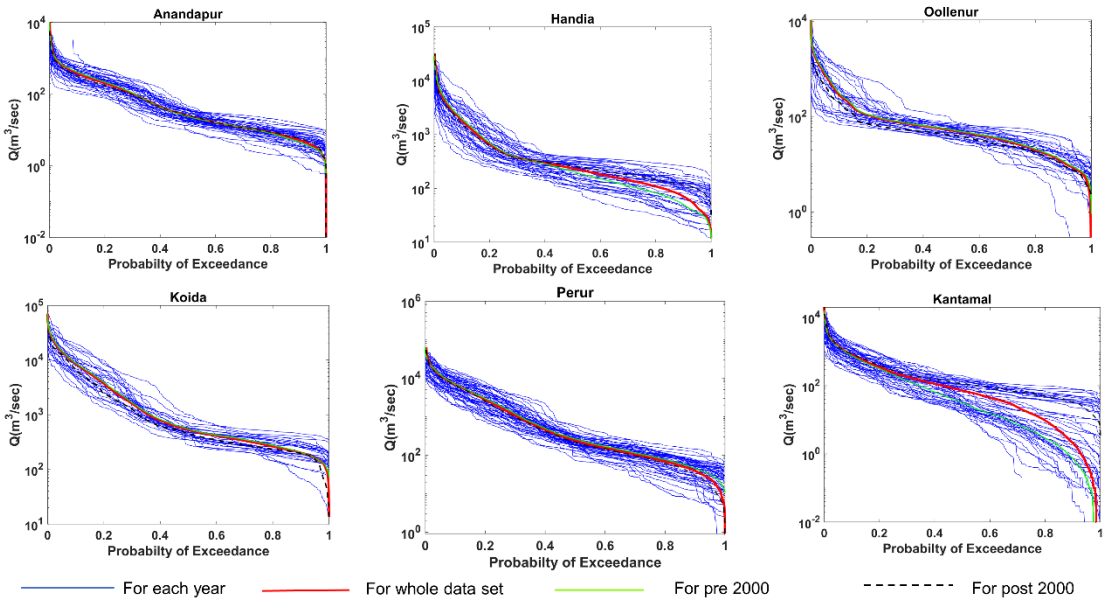

Figure S2. Flow duration curve (FDC) for selected rivers. The FDC for each year during the observation period is shown in blue lines. The FDC in red shows the entire records considering all available records. The FDC for the pre-2000 (1965 – 2000) time window is shown in green, whereas FDC for the post-2000 (2001-2018) is shown in black dashed line. The variations in the FDC indicates the flow properties and storage availability in the catchment. Further, they show the influence of basin geology and climate on the streamflow variability.

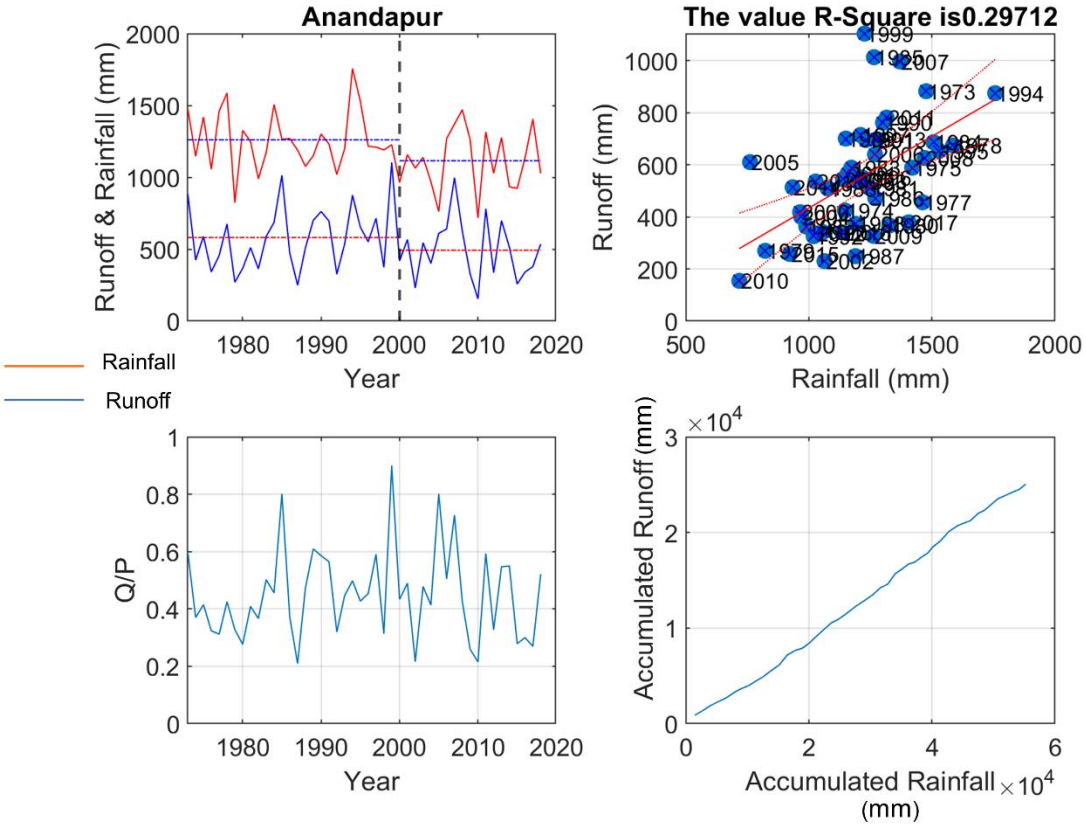

Figure S3. Graphical assessment of rainfall versus runoff for the selected river basin, Anandpur (21.21°N-86.12°E), at Baitarni River basin, in Odhisa. (Top panel; left) compares the temporal variability in rainfall versus runoff time series during the period of records availability. (Top panel – *right*) shows the scatter plot of annual average rainfall versus annual average runoff showing the degree of association between the two time series. The each year is shown using circles in blue. (Bottom panel - *left*) shows the streamflow elasticity (annual average streamflow, *Q*/basin averaged rainfall, *P*). (Bottom panel – *right*) compares the accumulated rainfall versus accumulated runoff using double mass curve, showing the degree of consistency between the two time series.

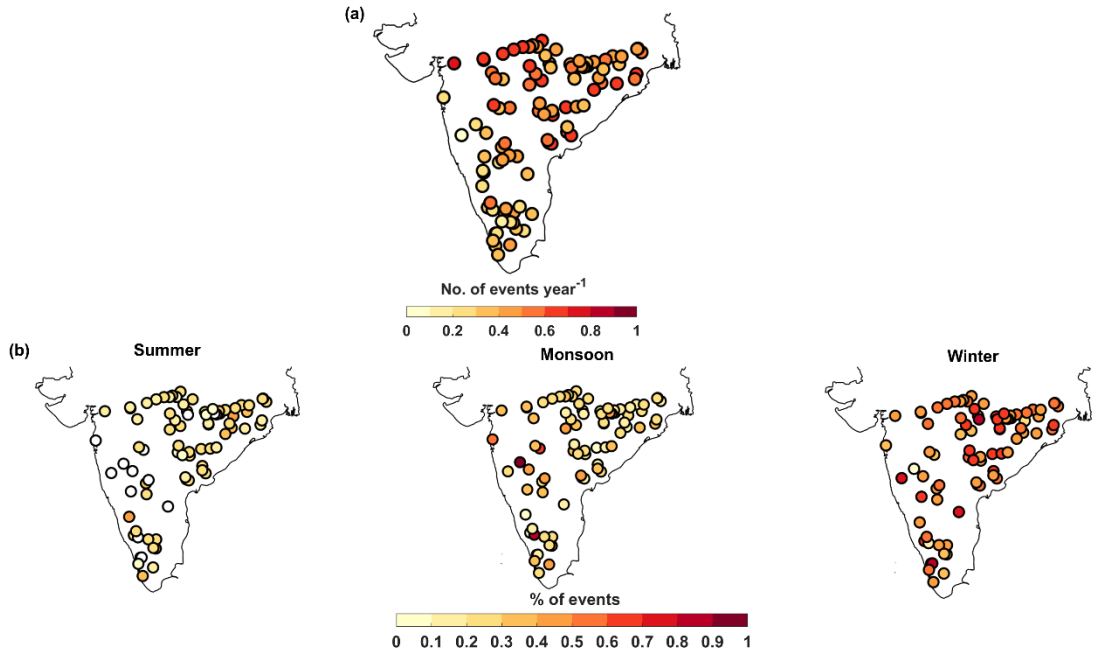

Figure S4. Frequency of droughts (number of events) per year. (a) Average number of droughts per year without accounting for seasonal stratifications. (b) The percentage occurrence of droughts during different seasons.

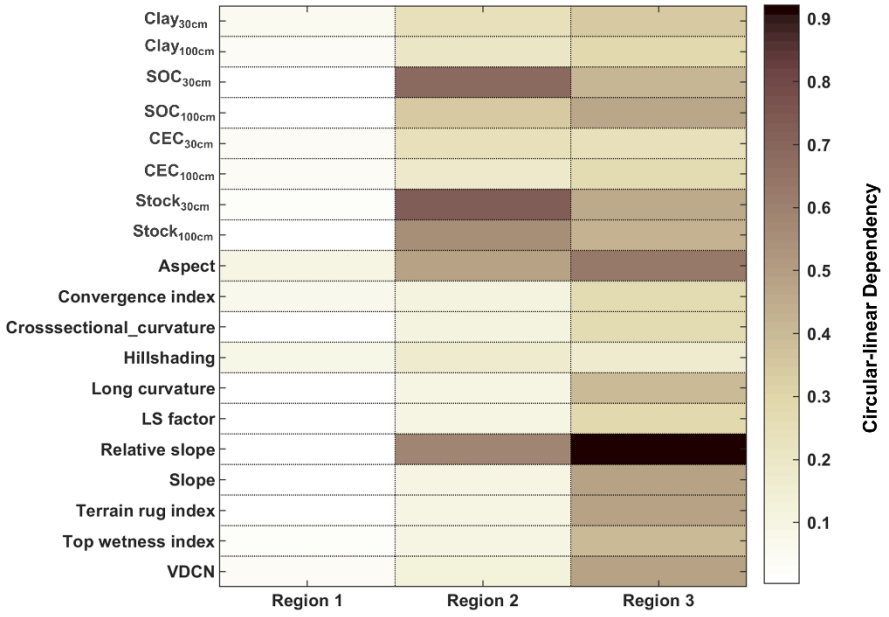

Figure S5. Circular-linear dependency of catchment controls and the time of onset of streamflow drought. The heatmap shows the non-linear dependence between different catchment and soil properties for three distinct regions.

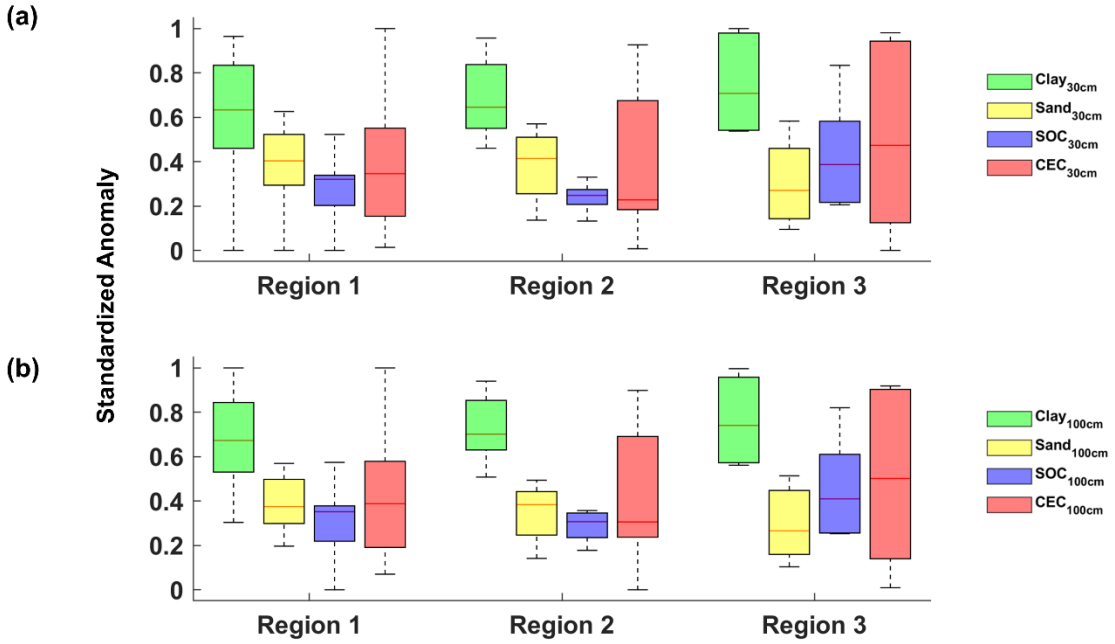

Figure S6. Soil properties across different regions. (a) Box plots showing standardized anomaly of soil properties at (a) 30 cm- and (b) 100 cm-depth. The y-axis shows the standardized spatial anomaly for each region. The median value of standardized anomaly is represented using the horizontal line within the box plot. Box bottom and top edges show 25th and 75th percentiles, respectively, whereas the spread of the boxes indicates interquartile range.

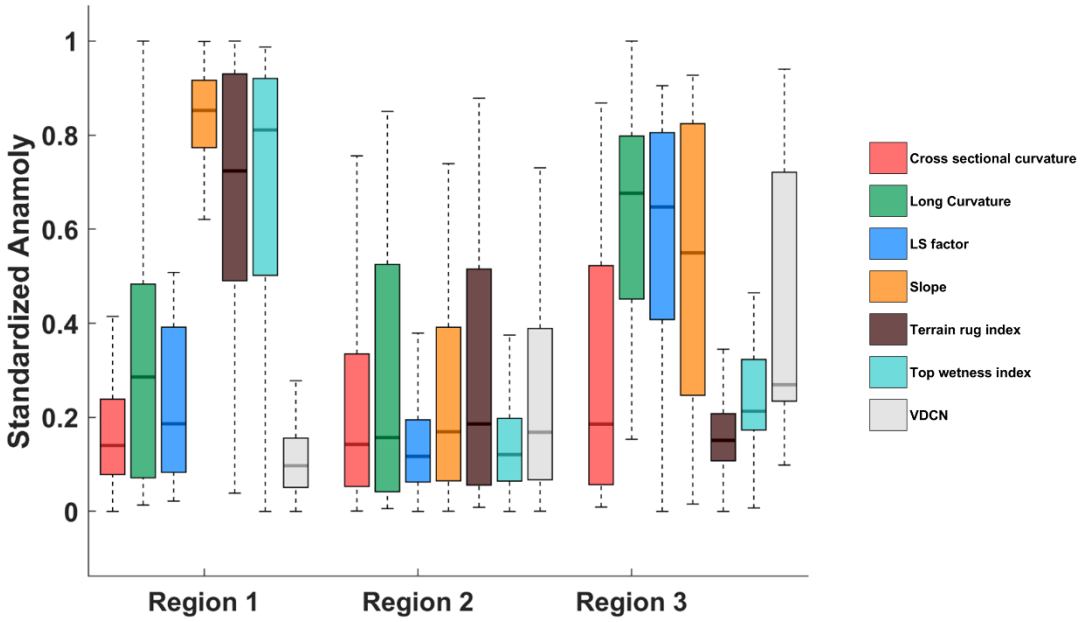

Figure S7. Variations in catchment properties across different regions. The y-axis shows the standardized spatial anomaly for each region. Shades in the boxplot denote catchment properties.

Table S1. Details of selected basins, station locations, catchment area and data available period

River	Station	Latitude (ºN)	Longitude (ºE)	Area (km^2)	Starting year	Ending year
Baitarni	Ananadpur	21.2089	86.1233	8570	1973	2018
Bharathapuzha	Mankara	10.7611	76.4861	2775	1986	2018
Bharathapuzha	Pudur	10.78	76.575	1313	1986	2018
Brahmani	Jenapur	20.8897	86.0142	33955	1990	2018
Brahmani	Gomlai	21.8378	84.9425	21950	1980	2018
Brahmani	Tilga	22.3333	84.5042	3160	1980	2018
Brahmani	Jaraikela	22.3217	85.1047	9160	1973	2018
Cauvery	Musiri	10.9433	78.435	66243	1974	2011
Cauvery	Kodumudi	11.0811	77.8903	53233	1972	2016
Cauvery	Urachikottai	11.4778	77.7	44100	1980	2018
Cauvery	Biligundulu	12.18	77.73	36682	1972	2018
Cauvery	Kollegal	12.1892	77.1	21082	1972	2018
Cauvery	Kudige	12.5025	75.9611	1934	1974	2018
Cauvery	Savandapur	11.5217	77.51	5776	1979	2018
Cauvery	Thengumarahada	11.5728	76.9192	1370	1980	2018
Cauvery	T.K. Halli	12.4167	77.1925	7890	1979	2015
Cauvery	K.M.Vadi	12.3422	76.2875	1330	1980	2015
Cauvery	M.H. Halli	12.8189	76.1333	3050	1979	2018
Godavari	Perur	18.5872	80.3958	268200	1966	2015
Godavari	Mancherial	18.8358	79.4447	102900	1967	2014
Godavari	Yelli	19.0439	77.4556	53630	1979	2011
Godavari	G.R. Bridge	19.0206	76.7264	33934	1977	2013
Godavari	Dhalegaon	19.2203	76.3633	30840	1966	2007
Godavari	Pathagudem	18.8525	80.3494	40000	1966	2008
Godavari	Chindnar	19.0794	81.3011	17270	1972	2013
Godavari	Jagdalpur	19.1081	82.0228	7380	1966	2011
Godavari	Nowrangpur	19.1975	82.5119	3545	1966	2011
Godavari	Bhatpalli	19.3303	79.5042	3100	1987	2018
Godavari	Nandgaon	20.5344	78.8114	4580	1987	2018
Godavari	Pauni	20.7947	79.6478	35520	1965	2005
Godavari	Kumhari	21.8842	80.175	8070	1987	2018
Godavari	Keolari	22.3819	79.9	2970	1989	2014
Godavari	Satrapur	21.2167	79.2331	11100	1987	2017
Godavari	Ramakona	21.7189	78.8242	2500	1987	2016

Godavari	Rajegaon	21.6256	80.2539	5380	1987	2018
Godavari	Somanpally	18.6197	79.8069	12691	1967	2013
Godavari	Polavaram	17.2519	81.6564	307800	1966	2018
Godavari	Konta	17.7989	81.3928	19550	1966	2013
Godavari	Koida	17.4825	81.3867	305460	1978	2005
Krishna	Wadenapalli	16.7889	80.1314	235544	1966	2018
Krishna	Huvinhedgi	16.4906	76.92	55150	1977	2016
Krishna	Keesara	16.7156	80.3164	9854	1965	2015
Krishna	Paleru Bridge	16.9489	80.0478	2928	1966	2002
Krishna	Bawapuram	15.8833	77.9572	67180	1966	2015
Krishna	Mantralayam	15.9483	77.4264	60630	1973	2015
Krishna	Oollenur	15.4917	76.7169	33018	1973	2002
Krishna	Haralahalli	14.8261	75.6731	14582	1967	2015
Krishna	T. Ramapuram	15.6578	76.9647	23500	1966	2006
Krishna	Marol	14.9389	75.6181	4901	1967	2012
Krishna	Shimoga	13.9269	75.585	2831	1973	2016
Krishna	Yadgir	16.7375	77.1253	69863	1966	2010
Krishna	Takli	17.4131	75.8478	33916	1966	2000
Krishna	Narasingpur	17.9728	75.1397	22856	1967	2010
Krishna	Cholachguda	15.87	75.725	9373	1984	2006
Krishna	Warunji	17.2717	74.1656	1890	1967	2009
Mahanadi	Andhiyarkore	21.8325	81.60389	2210	1978	2016
Mahanadi	Baronda	20.91111	81.88472	3225	1979	2017
Mahanadi	Hirakud	21.51833	83.85361	83400	1991	2011
Mahanadi	Tikarapara	20.60167	84.77583	124450	1973	2018
Mahanadi	Basantpur	21.72194	82.78944	57780	1972	2018
Mahanadi	Seorinarayan	21.715	82.59639	48050	1986	2017
Mahanadi	Rajim	20.975	81.87778	8760	1972	2014
Mahanadi	Kantamal	20.6525	83.72333	19600	1972	2018
Mahanadi	Kesinga	20.20444	83.22222	11960	1979	2018
Mahanadi	Salebhata	20.97833	83.55139	4650	1974	2017
Mahanadi	Sundargarh	22.11361	84.00861	5870	1978	2018
Mahanadi	Kurubhata	21.97833	83.21361	4625	1979	2018
Mahanadi	Bamnidhi	21.89778	82.71389	9730	1972	2018
Mahanadi	Rampur	21.65528	82.52139	2920	1972	2017
Mahanadi	Jondhra	21.71306	82.35833	29645	1980	2018
Mahanadi	Simga	21.62694	81.69167	30761	1972	2016
Mahanadi	Ghatora	22.04194	82.22278	3035	1980	2018
Muvattupuzha	Ramamangalam	9.9406	76.4744	1342	1979	2018

Narmada	Mohgaon	22.7608	80.6236	3919	1981	2018
Narmada	Patan	23.3111	79.6619	3950	1980	2017
Narmada	Belkheri	22.9289	79.3394	1508	1978	2017
Narmada	Barmanghat	23.0297	79.0158	26453	1972	2012
Narmada	Gadarwara	22.9228	78.7908	2270	1978	2018
Narmada	Sandia	22.9158	78.3475	33953	1979	2014
Narmada	Hoshangabad	22.7561	77.7328	44548	1973	2014
Narmada	Handia	22.4917	76.9936	54027	1978	2018
Narmada	Kogaon	22.1014	75.6842	3919	1979	2017
Narmada	Mandleshwar	22.1683	75.6608	72809	1974	2018
Narmada	Garudeshwar	21.885	73.6544	87892	1973	2016
Pampa	Malakkara	9.3325	76.6631	1713	1986	2018
Pennar	Alladupalli	14.7172	78.6686	8758	1986	2018
Periyar	Arangaly	10.2814	76.3153	1342	1979	2018
Ponnaiyar	Vazhavachanur	12.0667	78.9775	10780	1979	2006
Ponnaiyar	Gummanur	12.555	78.1386	4620	1979	2018
Subarnarekha	Ghatsila	22.5806	86.4683	14176	1972	2014
Subarnarekha	Jamshedpur	22.8156	86.2161	12649	1973	2014
Subarnarekha	Adityapur	22.7914	86.1736	6309	1972	2018
Tapi	Burhanpur	21.2994	76.235	8487	1973	2017
Tapi	Gopalkheda	20.8742	76.9897	9500	1978	2016
Tapi	Yerli	20.9358	76.4756	16517	1974	2017
Vaigai	Theni	10.0011	77.485	1200	1979	2018
Vaitarna	Durvesh	19.7131	72.93	2019	1972	2018

Table S2. Details of station that were distracted due to low rainfall-runoff correlation

River	Station	Latitude (°N)	Longitude (°E)	Area (km^2)	Rainfall-Runoff Correlation
Cauvery	Musiri	10.9433	78.435	66243	0.006
Cauvery	Kodumudi	11.0811	77.8903	53233	0.019
Cauvery	Thengumarahada	11.5728	76.9192	1370	0.012
Cauvery	T.K. Halli	12.4167	77.1925	7890	0.025
Godavari	Yelli	19.0439	77.4556	53630	-0.02
Krishna	Bawapuram	15.8833	77.9572	67180	0.011
Krishna	Mantralayam	15.9483	77.4264	60630	0.015
Krishna	Oollenur	15.4917	76.7169	33018	0.039
Krishna	Haralahalli	14.8261	75.6731	14582	0.021
Krishna	Marol	14.9389	75.6181	4901	0.012
Muvattupuzha	Ramamangalam	9.9406	76.4744	1342	0.033
Ponnaiyar	Vazhavachanur	12.0667	78.9775	10780	0.025
Ponnaiyar	Gummanur	12.555	78.1386	4620	-0.009
Tapi	Gopalkheda	20.8742	76.9897	9500	-0.021
Tapi	Yerli	20.9358	76.4756	16517	-0.049

Table S3. Details of soil and catchment properties used for attribution of static controls

Variable Name	Abberviation	Unit	Variable Type
Clay content at 30 and 100 cm depth	$Clay_{30cm}$ $Clay_{100cm}$	Percentage (%)	Soil
Soil organic carbon at 30 and 100 cm depth	SOC_{30cm} SOC_{100cm}	Percentage (%)	Soil
Cation exchange capacity at 30 and 100 cm depth	CEC_{30cm} CEC_{100cm}	cmol/kg	Soil
Stock at 30 and 100 cm depth	$Stock_{30cm}$ $Stock_{100cm}$	t/ha	Soil
Aspect	-	radian	Catchment
Convergence Index	-	-	Catchment
Cross sectional curvature	-	m^{-1}	Catchment
Hill shading	-	radian	Catchment
Longitudinal curvature	Long curvature	m^{-1}	Catchment
Slope length gradient factor	LS factor	-	Catchment
Relative slope	-	-	Catchment
Slope	-	Radian	Catchment
Terrain rug index	TRI	-	Catchment
Topographic wetness index	TWI	-	Catchment
Vertical distance to channel network	VDCN	M	Catchment

References

Burn, D. H., & Whitfield, P. H. (2018). Changes in flood events inferred from centennial length streamflow data records. *Advances in Water Resources*, *121*, 333–349. https://doi.org/10.1016/j.advwatres.2018.08.017

Chen, L., Singh, V. P., Guo, S., Fang, B., & Liu, P. (2012). A new method for identification of flood seasons using directional statistics. *Hydrological Sciences Journal*, *58*(1), 28–40. https://doi.org/10.1080/02626667.2012.743661

Ranstam, J. (2016). Multiple P -values and Bonferroni correction. *Osteoarthritis and Cartilage*, *24*(5), 763–764. https://doi.org/10.1016/j.joca.2016.01.008